Journal of Solid State Chemistry **148,** 295–301 (1999)
Article ID jssc.1999.8450, available online at http://www.idealibrary.com on IDEAL®

Crystal Structure and Physical Properties of $BiCoPO_5$

Said Nadir,[1] J. S. Swinnea, and H. Steinfink

Texas Materials Institute and Department of Chemical Engineering, University of Texas, Austin, Texas 78712

Received March 1, 1999; in revised form June 30, 1999; accepted July 22, 1999

$BiCoPO_5$ is isostructural with $BiNiPO_5$, $a = 7.253(1)$ Å, $b = 11.294(1)$ Å, $c = 5.230(1)$ Å, $\beta = 107.82(1)^\circ$, $P2_1/n$, $z = 4$, R_1 $[I > 2\sigma(I)] = 0.025$, R_1 for all reflections = 0.030. Co is in a slightly distorted octahedral coordination with Co–O bonds ranging from 2.007(5) to 2.150(5) Å. Bi is in six-fold coordination to oxygen in a distorted octahedral coordination with Bi–O bonds ranging from 2.129(4) to 2.693(5) Å. The lone-pair electrons are 0.39 Å from the Bi nucleus. The PO_4 tetrahedron is quite regular with P–O bonds 1.532(5)–1.558(5) Å. Phases in the solid solution series $BiNi_{1-x}Co_xPO_5$, $0 \le x \le 1$ are monoclinic. Magnetic susceptibility measurements show that they are all antiferromagnets with T_N varying from 20 K for the pure Ni phase to 15 K for pure Co. The materials are semiconductors with $E_g = 0.38$ ev and $E_g = 0.9$ ev for the Ni and Co compounds, respectively. When monoclinic $BiCoPO_5$ is heated past the melting point to 950°C it decomposes and an orthorhombic phase is formed. Single crystal Weissenberg photographs of this new phase yield lattice parameters $a = 14.688(3)$ Å, $b = 11.229(2)$ Å, $c = 5.438(1)$ Å, space group *Ibam* or *Iba*2.

INTRODUCTION

The discovery that $Bi_4V_2O_{11}$ is a good oxide ion conductor has led to intense research on this and related compounds. Numerous attempts have been reported to improve the ion conductivity by isovalent and aliovalent substitution of the transition metal and of bismuth. The Bi–P(V)–O systems (1–4) and the pseudoternary systems Bi_2O_3–PbO–M_2O_5, where M = P, V, A, have been extensively investigated (5–7) in the expectation that some of the compounds will display interesting physical properties such as improved anionic conduction. Similarly the phase diagram Bi_2O_3–NiO–PO_5 was explored toward that same goal (8). Recently the crystal structure of Pb_4BiPO_8 (9) has been determined and it shows a close relationship to Pb_5SO_8 (10). The investigation of Bi and Pb compounds has the added interest that structural modifications are introduced in the coordination polyhedra due to the nonbonding $6s^2$ electron pair (11–16).

Only one line compound, $BiNiPO_5$, is reported in the Bi_2O_3–NiO–P_2O_5 system. It crystallizes in the monoclinic space group $P2_1/n$ and melts congruently at 1040°C (8). Ketatni (17) attempted to synthesize the analogous $BiCoPO_5$ compound but mentions that instead an orthorhombic phase is observed. Its crystal structure, however, was not determined. We undertook the study of the solid solution series $BiNi_{1-x}Co_xPO_5$ to see the influence of Co on the crystal structure and on the magnetic and electrical properties and to determine the crystal structure of the monoclinic compound $BiCoPO_5$ from single-crystal X-ray diffraction data.

EXPERIMENTAL

The syntheses were carried out by mixing Bi_2O_3 (Strem Chemicals, 99.9% Bi), which was preheated at 600°C to remove carbonates, Co(II,III) oxide (Alfa Aesar 99.7% Co), NiO (Alfa Aesar 99% Ni), and $(NH_4)H_2PO_4$ (GFS Chemicals 99.5%) in the desired stoichiometric amounts. The mixtures were thoroughly ground in an agate mortar, heated initially to 300°C and then held at 500°C overnight to decompose $(NH_4)H_2PO_4$. To ensure homogeneous specimens, heating at 850°C for 3 days with intermittent grindings completed the syntheses. The samples were quenched in air. Identification was done by powder X-ray diffraction using Cu$K\alpha$ radiation and equipment with a variable slit system and a diffracted-beam graphite monochromator. Density measurements were done in a helium displacement pycnometer. Two-probe impedance spectroscopy was used to measure the ac conductivity of sintered pellets. The pellets were wet-sanded before applying silver paint for electrical contacts. A Hewlett-Packard 4192 AIF impedance analyzer was used for measurements over a frequency range 5 to 13 MHz, an ac amplitude of 40 mV, and a temperature interval $300 \le T \le 700$°C with an accuracy of ± 1.5°C. Magnetic susceptibilities were measured with a Quantum-Design DC SQUID magnetometer. The specimen was equilibrated at 35 K in zero field. A field of 200 Oe was applied

[1] Present address: Département de Chemie, Faculté des Sciences BP 20, Universite Chouaib Doukkali, El jadida, Morocco.

0022-4596/99 $30.00

and measurements were taken to 320 K. The sample was held at that temperature and in the field for 1 h before measurements were continued to 5 K.

DISCUSSION

For the solid solution $BiNi_{1-x}Co_xPO_5$, $0 \leq x \leq 1$, the phases are monoclinic. In Table 1 are shown least squares refined lattice parameters obtained from the powder patterns and measured densities for selected compositions. Even though the ionic radii of Ni^{2+} and Co^{2+} are the same the atomic volume of Co is slightly greater and this is reflected in the slight increases of the cell parameters and cell volumes with increasing Co content. The powder X-ray patterns of the complete range of solid solutions show that they are isostructural. Ketatni (17) synthesized polycrystalline $BiCoPO_5$ and from the powder pattern showed that it is most likely isostructural with $BiNiPO_5$. He was unable to grow single crystals and we, therefore, grew these crystals by melting the powder at 910°C, slow cooling to 400°C, followed by air quenching. Initial atomic parameters were obtained by the direct method and refined by least squares with the computer program SHELX93 (18) incorporated in the program WINGX (19). Table 2 lists the conditions for the crystallographic data collection and results of the structure refinement. Atomic coordinates and isotropic displacement parameters are shown in Table 3a and anisotropic parameters in Table 3b. Table 4 contains a listing of interatomic distances and angles.

Differential thermal analysis (DTA) of $BiCoPO_5$ does not show a phase transformation between room temperature and the melting point, $\approx$900°C, and high temperature powder X-ray diffraction confirmed that result. The recrystallized melt exhibited the same powder pattern as the original material. However, when $BiCoPO_5$ was heated at 950°C and slow cooled to 400°C numerous deep violet crystals with an acicular habit were observed as well as some light, violet colored, platy crystals of the monoclinic phase. A single crystal of this new phase was selected and Weissenberg and precession photographs showed orthorhombic symmetry, $a = 14.69$ Å, $b = 11.286$ Å, $c = 5.422$ Å, with extinctions consistent with space groups *Ibam* or *Iba*2. Table 5 lists the *d* spacings for both phases. Nearly all of the powder diffraction lines of the orthorhombic phase could be indexed with the orthorhombic parameters except for a few lines with small intensities, indicative of the monoclinic phase. Evidently at 950°C decomposition to a new phase occurred. Ketatni (17) reacted precursors in the ratio 2 Bi:Co:P and found in the product Co_3O_4, violet needles that turned out to be the orthorhombic phase, and $Bi_{6.67}P_4O_{20}$ (20). Single crystal data from the violet needles yielded essentially the same parameters and the same possible space groups that we found. Their attempts to solve the structure yielded the Bi and Co positions but no further progress was possible. He ascribed this inability

TABLE 1
Least Squares Refined Lattice Parameters, Å, and Densities, g/cm³, of the Monoclinic Phases $BiNi_{1-x}Co_xPO_5$

Composition, x	0[a]	0.25	0.50	0.75	1
a	7.166(1)	7.189(1)	7.204(1)	7.215(2)	7.253(1)
b	11.206(5)	11.230(2)	11.248(2)	11.261(2)	11.294(1)
c	5.173(5)	5.188(1)	5.203(1)	5.215(1)	5.230(1)
β°	107.281(6)	107.43(1)	107.57(1)	107.74(2)	107.82(1)
V	396.72(4)	399.62(2)	401.94(1)	403.56(2)	407.87(1)
ρ_{mes}	6.326	6.321(6)	6.365(8)	6.284(3)	6.309(1)
ρ_{cal}	6.339(6)	6.294(3)	6.258(2)	6.234(3)	6.169(2)

[a] Ref. (8).

TABLE 2
Crystal Data and Structure Refinement for Monoclinic $BiCoPO_5$

Formula	$BiCoPO_5$
Formula weight	378.88
Temperature, K	293
Wavelength, Å	0.71073
Space group	$P2_1/n$
Unit cell dimensions, Å, angles, deg.	
a	7.238(1)
b	11.270(2)
c	5.217(1)
β°	107.84(3)
Volume, Å³	405.1(1)
Z, density (g/cm³) obs/calc	4, 6.309(1)/6.169(2)
Color/habit	Light violet/tabular
Diffractometer	CAD4
Scan method	ω–2θ
Absorption coefficient mm^{-1}	47.773
$F(000)$	660
Crystal size/mm	$\bar{1}$ 1 1/0.011, 1 $\bar{1}$ $\bar{1}$/0.011, 2 $\bar{3}$ 1/0.056, $\bar{1}$ $\bar{1}$ $\bar{1}$/0.064, $\bar{1}$ $\bar{2}$ 0/0.066, 0 $\bar{1}$ 1/0.09
θ range, degrees	3.47 to 29.95
Limiting indices	$-10 \leq h \leq 10$, $-15 \leq k \leq 0$, $-7 \leq l \leq 7$
Reflections collected/unique	2350/1179
R(int)	0.0658
Refinement method, F^2	Full-matrix least-squares
Data/restraints/parameters	1179/0/49
GOF F^2	1.055
R [$I > 2\sigma(I)$]	$R_1 = 0.0250$, w$R_2 = 0.0593$
R (all data)	$R_1 = 0.0295$, w$R_2 = 0.0611$
Extinction coefficient	0.0175(6)
Largest diff. peak and hole e Å^{-3}	2.511, -1.253

TABLE 3a
Atomic Coordinates and Equivalent Isotropic Displacement Parameters ($Å^2 \times 10^3$) for Monoclinic $BiCoPO_5$

	X	*Y*	*Z*	*U*(eq)[a]
Bi	0.1904(1)	0.0981(1)	0.1131(1)	8(1)
Co	0.8132(1)	0.0838(1)	0.3717(2)	8(1)
P	0.0210(2)	0.3485(1)	0.2158(3)	6(1)
O(1)	0.1627(7)	0.4186(4)	0.4477(9)	10(1)
O(2)	− 0.0118(7)	0.2244(4)	0.3136(9)	12(1)
O(3)	− 0.1689(8)	0.4188(4)	0.1095(9)	14(1)
O(4)	0.9823(6)	0.0229(4)	0.7453(8)	9(1)
O(5)	0.1094(7)	0.3276(4)	− 0.0178(9)	14(1)
P	− 0.7764	0.1257	0.1357	

[a] Defined as one third of the trace of the orthogonalized U_{ij} tensor.
Note. The Lp row lists the coordinates of the lone-pair electrons for Bi.

to the possibility of twinning or to a bad absorption correction.

The lattice parameters of the two phases are very similar but the monoclinic *a*-axis is about $\frac{1}{2}$ of that of the orthorhombic phase, suggesting that the two structures might be related. The monoclinic compound could usually be prepared phase-pure. Occasionally a diffraction line was observed that later was identified as the most intense line of the orthorhombic phase. If this line was included with the lines of the monoclinic compound, TREOR (21) provided lattice parameters $a = 14.491(2)$ Å, $b = 11.282(2)$ Å, $c = 5.2249(7)$ Å, $\beta = 107.85(1)^\circ$, $F_{30} = 32(0.00926, 100)$ (22), a "new" monoclinic phase. However, the omission of this one line leads to the standard lattice parameters of the monoclinic phase. Ketatni (17) reports the same information.

The crystal structure of BiCoPO5 is isostructural with BiNiPO5 (8) and is shown in Fig. 1. Bi is coordinated to six oxygen ions. Sharing two O(4) ions forms a binuclear unit Bi_2O_{10}. The angle O(4)–Bi–O(4) is 74.9(2)°. The Co atoms similarly form a binuclear unit Co_2O_{10} by sharing two O(4) ions but from different Bi_2O_{10} moieties. The Co and PO_4 groups serve to tie Bi_2O_{10} units into a three-dimensional framework. The Bi–O bond lengths vary from 2.129 to 2.693 Å. Co is in the octahedral and the PO_4 ion in the usual tetrahedral coordination. Bond lengths and angles are shown in Table 4.

While preparing mixtures of the solid solution series $BiNi_{1-x}Co_xPO_5$ we also prepared mixtures $BiCo_{1+x}PO_5$ with $x > 1$ but the powder X-ray diffraction patterns show the monoclinic phase $BiCoPO_5$ and Co_3O_4. Ketatni reports the same result (17). It is noteworthy that the orthorhombic phase was obtained from the melt of monoclinic $BiCoPO_5$ that was raised to 950°C. We also obtained the orthorhombic compound when reacting mixtures that were richer in Co and deficient in P than required for $BiCoPO_5$. The powder X-ray diffraction diagram of the product resulting from a mixture of nominal stoichiometry Bi:2Co:0.65 (PO_4) showed the presence of the monoclinic and orthorhombic phases. The phase diagram in the vicinity of BiCo PO_5 needs further study and is now in progress.

TABLE 3b
Anisotropic Displacement Parameters ($Å^2 \times 10^3$) for Monoclinic $BiCoPO_5$[a]

	U_{11}	U_{22}	U_{33}	U_{23}	U_{13}	U_{12}
Bi	7(1)	8(1)	8(1)	0(1)	3(1)	− 1(1)
Co	7(1)	10(1)	7(1)	1(1)	3(1)	1(1)
P	7(1)	6(1)	7(1)	0(1)	3(1)	− 1(1)

[a] The exponential anisotropic displacement factor takes the form: $-2\pi^2 [h^2a^{*2}U_{11} + \ldots + 2hka^*b^*U_{12}]$.

TABLE 4
Bond Lengths, Å, and Angles, °, for Monoclinic $BiCoPO_5$

Bond		Angles	
		O(4)#1–Bi–O(4)#2	74.9(2)
Bi–O(4)#1	2.129(4)	O(4)#1–Bi–O(1)#3	80.4(2)
Bi–O(4)#2	2.213(4)	O(4)#2–Bi–O(1)#3	76.7(2)
Bi–O(1)#3	2.352(5)	O(4)#1–Bi–O(3)#4	71.7(2
Bi–O(3)#4	2.483(5)	O(4)#2–Bi–O(3)#4	145.9(2)
Bi–O(2)	2.491(5)	O(1)#3–Bi–O(3)#4	91.0(2)
Bi–O(5)	2.693(5)	O(4)#1–Bi–O(2)	74.8(2)
		O(4)#2–Bi–O(2)	104.56(15)
		O(1)#3–Bi–O(2)	153.7(2)
Co–O(5)#4	2.007(5)	O(3)#4–Bi–O(2)	73.2(2)
Co–O(4)	2.075(4)	O(4)#1–Bi–O(5)	126.7(2)
Co–O(2)#5	2.107(5)	O(4)#2–Bi–O(5)	96.3(2)
Co–O(4)#6	2.137(4)	O(1)#3–Bi–O(5)	149.8(2)
Co–O(1)#7	2.146(5)	O(3)#4–Bi–O(5)	109.01(15)
Co–O(3)#3	2.150(5)	O(2)–Bi–O(5)	56.43(15)
		O(5)#4–Co–O(4)	99.7(2)
		O(5)#4–Co–O(2)#5	101.2(2)
P–O(2)	1.532(5)	O(4)–Co–O(2)#5	100.2(2)
P–O(3)	1.535(5)	O(5)#4–Co–O(4)#6	175.5(2)
P–O(1)	1.542(5)	O(4)–Co–O(4)#6	79.7(2)
P–O(5)	1.558(5)	O(2)#5–Co–O(4)#6	83.3(2)
		O(1)#7–Co–O(3)#3	86.3(2)
O(2)–P–O(3)	112.2(3)	O(5)#4–Co–O(1)#7	96.7(2)
O(2)–P–O(1)	109.9(3)	O(4)–Co–O(1)#7	158.6(2)
O(3)–P–O(1)	109.0(3)	O(2)#5–Co–O(1)#7	89.9(2)
O(2)–P–O(5)	105.3(3)	O(4)#6–Co–O(1)#7	82.9(2)
O(3)–P–O(5)	109.4(3)	O(5)#4–Co–O(3)#3	90.4(2)
O(1)–P–O(5)	110.9(3)	O(4)–Co–O(3)#3	80.0(2)
		O(2)#5–Co–O(3)#3	168.1(2)
		O(4)#6–Co–O(3)#3	85.1(2)
		O(1)#7–Co–O(3)#3	86.3(2)

Note. Symmetry transformations: #1, $-x+1; -y, -z+1$; #2, $x-1, y, z-1$; #3, $-x+1/2, y-1/2, -z+1/2$; #4, $x+1/2, -y+1/2, z+1/2$; #5, $x+1, y, z$; #6, $-x+2, -y, -z+1$; #7, $x+1/2, -y+1/2, z-1/2$.

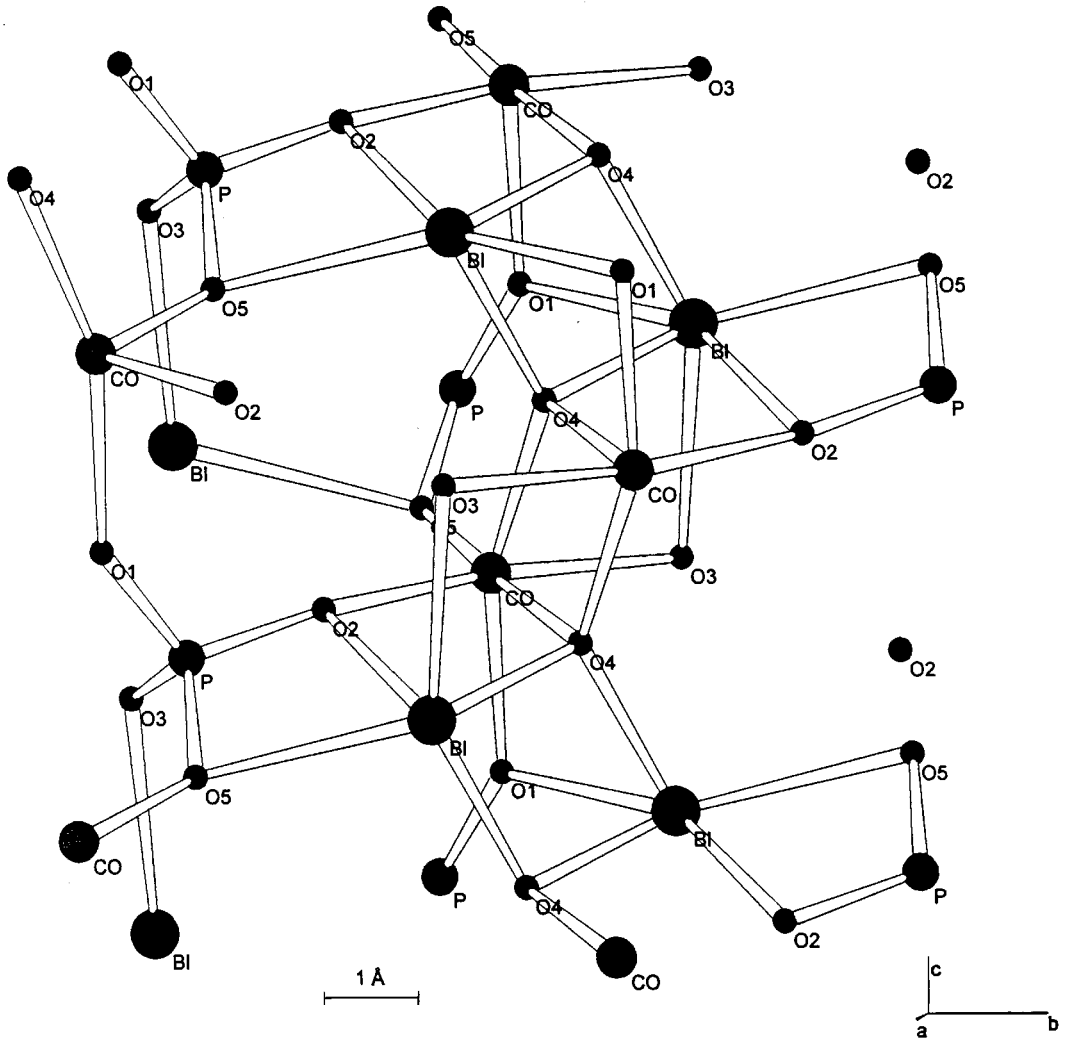

FIG. 1. The crystal structure of $BiCoPO_5$. Two *c*-axis periodicities are shown.

LONE-PAIR LOCALIZATION

The interplay among lone-pair electrons, stereochemistry, and crystal structure has long been of interest to crystallographers and solid state chemists, (4, 15, 23). The theory enabling the calculation for localizing the lone-pair electrons in a crystal structure was developed by Verbaere *et al.* (13). It is based on the local electric field calculation in the whole crystal using Ewald's method (26) and was recently successfully applied to several materials (12, 15). It was incorporated in the computer program HYBRIDE (15). The mean ionicity for each *M* cation species was calculated for $BiCoPO_5$ from the electronegativity differences of the *M*–O bonds. Thus, a formal ionicity value was calculated for each bond using the formula

$$M\text{–O} = 1 - \exp[-(X_O - X_M)^2/4].$$

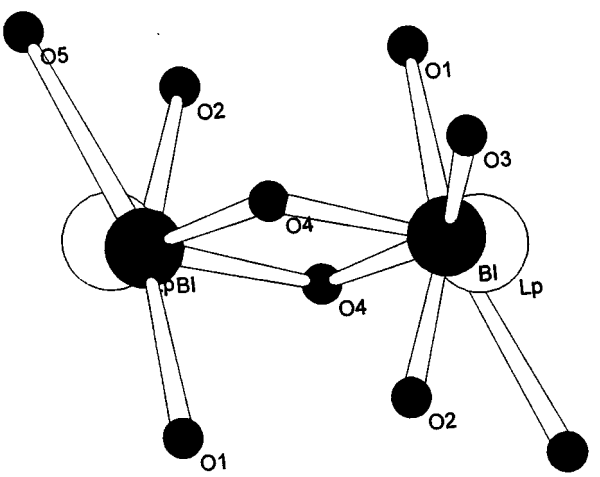

FIG. 2. The binuclear unit Bi_2O_{10} showing the lone-pair electrons, open circles.

TABLE 5
The Powder Patterns

h	k	l	$2\theta_{obs}$	$2\theta_{cal}$	d_{obs}	d_{cal}	I
			Monoclinic $BiCoPO_3$[a]				
1	1	0	15.206	15.217	5.8217	5.8175	5.2
0	2	0	15.851	15.871	5.5842	5.5794	11.8
−1	0	1	18.662	18.682	4.7509	4.7457	19.6
0	1	1	19.669	19.659	4.5098	4.5121	8.9
1	2	0	20.476	20.488	4.3338	4.3312	29.5
−1	2	1	24.000	23.995	3.7049	3.7056	32.4
2	0	0	24.523	24.523	3.6269	3.6271	1.3
1	1	1	25.942	25.971	3.4317	3.4280	12.3
1	3	0	26.441	26.447	3.3682	3.3674	59.0
−1	3	1	27.130	27.140	3.2841	3.2829	14.9
2	2	0	30.338	30.344	2.9437	2.9431	27.0
−2	2	0	30.502	30.504	2.9283	2.9281	12.5
−2	2	1	31.137	31.135	2.8700	2.8702	100.0
0	4	0	31.838	31.849	2.8084	2.8075	28.2
1	4	0	34.463	34.468	2.6002	2.5999	24.4
1	3	1	34.858	34.860	2.5717	2.5715	45.3
−1	1	2	35.437	35.440	2.5310	2.5308	44.3
0	4	1	36.738	36.739	2.4443	2.4442	18.0
2	1	1	36.978	36.956	2.4290	2.4303	37.2
0	1	2	37.121	37.128	2.4200	2.4195	29.5
−3	0	1	37.842	37.854	2.3755	2.3747	10.0
−2	1	2	38.527	38.537	2.3348	2.3342	7.8
3	1	0	40.138	40.122	2.2447	2.2456	26.7
2	4	0	41.443	41.451	2.1770	2.1766	27.5
−2	4	1	41.939	41.936	2.1524	2.1525	35.6
1	5	0	42.204	42.232	2.1395	2.1381	7.7
3	2	0	42.543	42.551	2.1232	2.1229	6.2
1	1	2	43.138	43.120	2.0953	2.0961	64.7
2	3	1	43.365	43.578	2.0849	2.0752	2.2
0	3	2	43.739	43.728	2.0679	2.0684	26.3
0	5	1	44.176	44.161	2.0484	2.0491	18.5
−2	3	2	44.976	44.963	2.0138	2.0144	14.6
−3	1	2	45.616	45.590	1.9871	1.9882	5.9
3	3	0	46.342	46.366	1.9576	1.9567	5.8
−3	2	2	47.798	47.793	1.9013	1.9015	8.7
0	6	0	48.480	48.487	1.8762	1.8759	26.1
3	1	1	49.222	49.222	1.8496	1.8496	6.7
−2	4	2	50.059	50.037	1.8206	1.8214	10.4
			Orthorhombic phase[b]				
0	2	0	15.785	15.685	5.6095	5.6450	7
0	1	1	18.292	18.141	4.8460	4.8861	2
2	1	1	21.804	21.829	4.0727	4.0682	15
1	2	1	23.547	23.528	3.7752	3.7781	4
4	0	0	24.170	24.215	3.6792	3.6725	2
3	2	1	29.236	29.206	3.0522	3.0553	100
4	1	1	30.698	30.423	2.9101	2.9357	6
5	1	0	31.451	31.437	2.8420	2.8433	59
0	4	0	31.890	31.675	2.8040	2.8225	12
0	0	2	32.899	33.026	2.7202	2.7100	18
1	1	2	34.486	34.552	2.5986	2.5937	7
6	0	0	36.608	36.675	2.4527	2.4483	7
4	3	1	38.079	38.017	2.3612	2.3650	7
5	3	0	38.906	38.855	2.3129	2.3158	4
3	4	1	40.591	40.434	2.2207	2.2290	19
1	3	2	41.446	41.485	2.1768	2.1749	6
5	1	2	46.153	46.240	1.9652	1.9617	16
0	4	2	46.454	46.412	1.9532	1.9548	21
2	4	2	47.931	48.128	1.8964	1.8891	4
7	2	1	49.304	49.238	1.8467	1.8490	15
2	6	0	50.054	49.995	1.8208	1.8228	7

[a] Cu$K\alpha$, $a = 7.253(1)$ Å, $b = 11.294(1)$ Å, $c = 5.230(1)$ Å, $\beta = 107.82°$.
[b] Cu$K\alpha$, $a = 14.688(3)$ Å, $b = 11.229(2)$ Å, $c = 5.438(1)$ Å.

The oxidation state of the cation was then multiplied by this factor to yield $+1.42$ for Bi^{3+}, $+1.03$ for Co^{+2}, and $+2.02$ for P^{5+}. The six oxygen atoms were given the balancing charge -0.89 to ensure electroneutrality within the lattice. The calculation of the lone-pair position placed them 0.39 Å from the nucleus of Bi (Table 3a and Fig. 2).

MAGNETIC AND ELECTRICAL PROPERTIES

Magnetic susceptibilities are shown in Fig. 3 for the solid solution of the monoclinic phases $BiNi_{1-x}Co_xPO_5$. They are all antiferromagnets. In Table 6 are shown the parameters of interest calculated from the Curie–Weiss law $\chi = C/(T - \theta)$. The μ_{eff} indicates the presence of high spin Ni^{2+}. For Co^{2+} the effective moment is due to spin–orbit coupling. The μ_{eff} behaves linearly with concentration. The antiferromagnetic interactions increase with increasing Co concentration but the Néel temperatures for the solid solutions are nearly constant and equal to that of the pure Co phase. The d electrons are more localized for the Co–O bond because of the greater ionicity than that of the Ni–O bond. This may be the reason for the stronger magnetic exchange for the Co phase even though the O–M–O angle is about 80° for both compounds. Measurements of the electrical conductivities for the Ni and Co phases over the range of 573 to 1073 K for the former and 773 to 1073 K for the latter show that they are semiconductors with activation energies $E_g = 0.38$ ev and 0.9 ev, respectively.

TABLE 6
Magnetic Parameters for Monoclinic $BiNi_{1-x}Co_xPO_5$

Composition, x	μ_{eff}, μ_B	θ (K)	T_N (K)
0	3.29	− 23	20
0.25	3.82	− 24	14
0.50	4.30	− 25	15
0.75	4.98	− 58	15
1.00	5.40	− 62	15

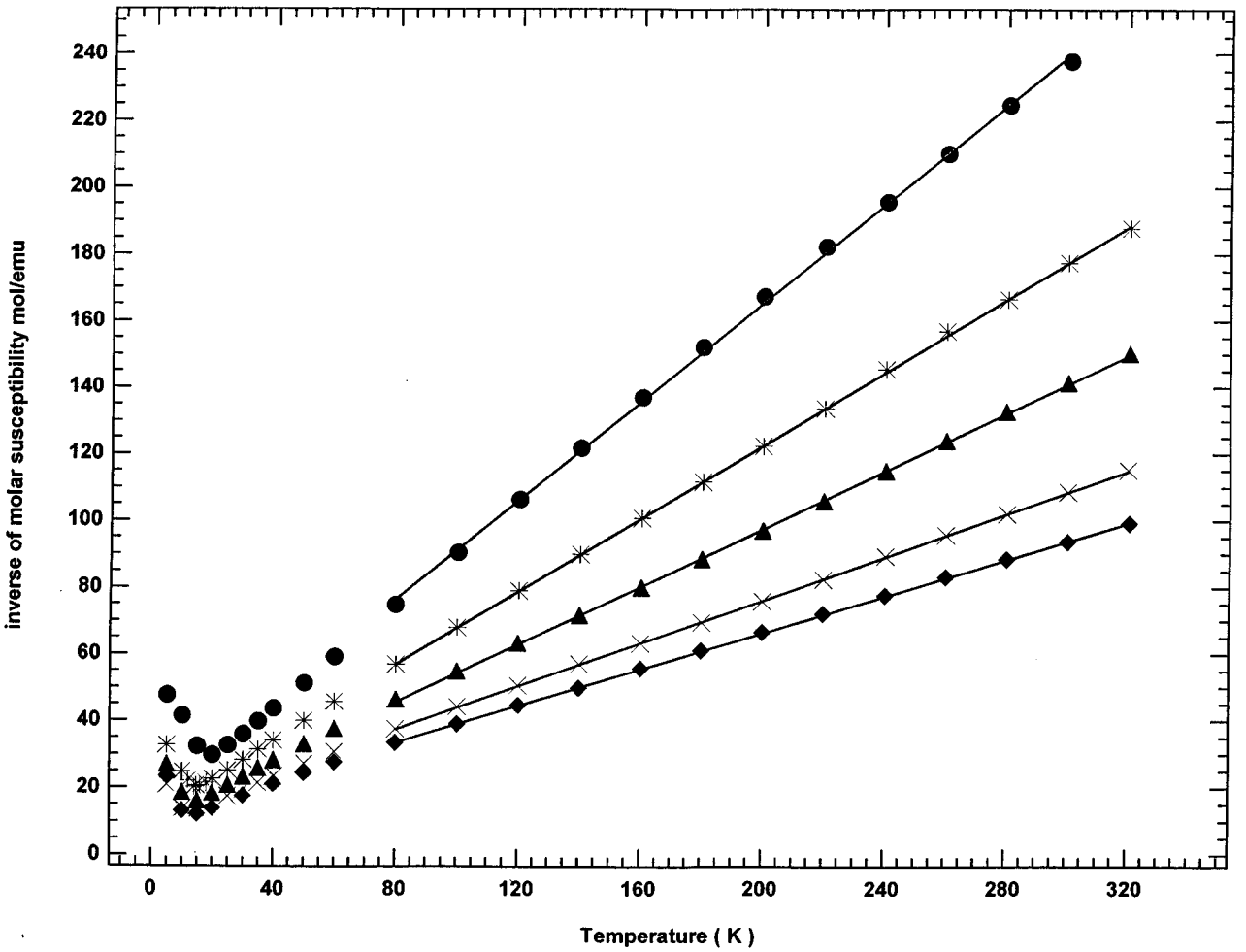

FIG. 3. The magnetic susceptibilities vs T for the monoclinic solid solutions $BiNi_{1-x}Co_xPO_5$. ●, $x = 0$; ✳, $x = 0.25$; ▲, $x = 0.5$; ×, $x = 0.75$; ◆, $x = 1$.

ACKNOWLEDGMENT

We gratefully acknowledge the support of the R. A. Welch Foundation of Houston, Texas.

REFERENCES

1. V. V. Volkov, L. A. Zhereb, Y. F. Kargin, V. M. Skorikov, and I. V. Tananeav, *Russ. J. of Inorg. Chem.* **28,** 1002 (1983).
2. J. P. Wignacourt, M. Drache, P. Conflant, and J. C. Boivin, *J. Chim. Phys.* **88,** 1933 (1991).
3. Y. A. Blinovskov and A. A. Fotiev, *Russ. J. Inorg. Chem.* **32,** 145 (1987).
4. A. Watanabe, *Solid State Ionics* **96,** 75 (1997).
5. A. Mizrahi, J. P. Wignacourt, M. Drache, and P. Conflant, *J. Mater. Chem.* **5**(6), 901 (1995).
6. Y. C. Jie and W. Eysel, *Powder Diffraction* **9,** 1 (1994).
7. A. Mizrahi, J. P. Wignacourt, and H. Steinfink, *J. Solid State Chem.* **133,** 516–521 (1997).
8. F. Abraham and M. Ketatni, *Eur. J. Solid State Inorg. Chem.* **32,** 429 (1995).
9. S. Giraud, J.-P. Wignacourt, M. Drache, G. Nowogrocki, and H. Steinfink, *J. Solid State Chem.* **142,** 80 (1999).
10. I. M. Steele and J. J. Pluth, *J. Electrochem. Soc.* **145,** 528 (1998).
11. O. Mentre, A.-C. Dhaussy, F. Abraham, and H. Steinfink, *J. Solid State Chem.* **140,** 417 (1998).
12. O. Mentre, A.-C. Dhaussy, F. Abraham, and H. Steinfink, *Chem. Mater.*, in press.
13. A. Verbaere, R. Marchand, and M. Tournoux, *J. Solid State Chem.* **23,** 383 (1978).
14. D. Le Bellac, J. M. Kiat, and P. Garnier, *J. Solid State Chem.* **114,** 459 (1995).
15. E. Morin, G. Wallez, S. Jaulmes, J. C. Couturier, and M. Quarton, *J. Solid State Chem.* **137,** 283 (1998).
16. L. Shimoni-Livny, J. P. Glusker, and C. W. Bock, *Inorg. Chem.* **37,** 1853 (1998).
17. M. Ketatni, Ph.D. dissertation. The University of Sciences and Technologies at Lille, France, April 1995.

18. G. M. Sheldrick, "SHELX93, Programs for the Refinement of Crystal Structures," Univ. of Göttingen, Germany.
19. L. J. Farrugia, "WINGX, ver. 1.61, An integrated system of windows programs for the solution, refinement and analysis of single crystal x-ray diffraction data." University of Glasgow, 1998.
20. F. Abraham, M. Ketatni, and G. Mairesse, *Eur. J. Solid State Inorg. Chem.* **31,** 313 (1994).
21. P. E. Werner, L. Eriksson, and M. Westdhal, *J. Appl. Cryst.* **18,** 367 (1985).
22. G. S. Smith and R. J. Snyder, *J. Appl. Cryst.* **12,** 60 (1979).
23. J. Galy and R. Enjalbert, *J. Solid State Chem.* **44,** 1 (1982).
24. N. Jakubowicz, O. Perez, D. Grebille, and H. Leligny, *J. Solid State Chem.* **139,** 194 (1998).
25. P. P. Ewald, *Ann. Phys.* **64,** 253 (1921).